DTU Library

Decentralized DLMPs with synergetic resource optimization and convergence acceleration

Pediaditis, Panagiotis; Ziras, Charalampos; Hu, Junjie; You, Shi; Hatziargyriou, Nikos

Published in:
Electric Power Systems Research

Link to article, DOI:
10.1016/j.epsr.2020.106467

Publication date:
2020

Document Version
Peer reviewed version

Decentralized DLMPs with synergetic resource optimization and convergence acceleration

Panagiotis Pediaditis[a,*], Charalampos Ziras[b], Junjie Hu[c], Shi You[b], Nikos Hatziargyriou[a]

[a]*School of Electrical and Computer Engineering, Technical University of Athens, Athens, Greece*
[b]*Department of Electrical Engineering, Technical University of Denmark, Lyngby, Denmark*
[c]*School of Electrical and Electronic Engineering, North China Electric Power University, Beijing, China*

Abstract

Dynamic pricing has been proposed for scheduling and controlling distributed energy resources (DERs) to mitigate operational problems in distribution networks. In this paper, we employ distribution locational marginal prices (DLMPs) to optimally schedule DERs, considering both line and voltage constraints. DLMPs are calculated in an iterative, decentralized manner to respect user privacy, using dual decomposition and the subgradient method. The inclusion of generating DERs in the problem formulation, and the nature of the subgradient method, may significantly increase the amount of required iterations. Recognizing the importance of convergence speed in such a mechanism, we act upon this by proposing a novel concept to identify and remove redundant constraints of the problem. The method is based on network topology observations in radial distribution networks. Redundant constraints are mapped to the respective Lagrange multipliers and are set to zero, thereby significantly increasing convergence speed. We validate our method in a 33 and a 136 bus system, showing the synergies of the co-optimization of generating and consuming DERs, and reducing the number of iterations at least threefold.

Keywords: Convergence speed, Distributed energy resources, Distribution network, DLMP, Decentralized optimization.

Nomenclature

Indices

i Aggregator

t Hour of day

k Iteration number

Parameters

*Corresponding author

Preprint submitted to Electric Power Systems Research *June 9,2020*

y_t	Predicted price
β_t	Price sensitivity parameter
c_t	Forecasted spot price
$B_{i,t}$	Block diagonal matrix of the price sensitivity parameter β_t
$\boldsymbol{e}_{i,t}^{\min}$	Lower limit for the SOC of the EVs
$\boldsymbol{e}_{i,t}^{\max}$	Upper limit for the SOC of the EVs
$\boldsymbol{p}_{i,t}^{\max}$	Upper limit for the charging power of EVs
$\hat{\boldsymbol{p}}_{i,t}^{\max}$	Upper limit for the curtailed power of DGs
$\underline{\boldsymbol{V}}, \overline{\boldsymbol{V}}$	Set of lower and upper voltage limits
$\underline{\boldsymbol{F}}, \overline{\boldsymbol{F}}$	Set of line loading lower and upper limits
$\boldsymbol{e}_i^{\text{init}}$	Set of initial SOC values
$\boldsymbol{d}_{i,t}$	Set of EV power demand
$\boldsymbol{P}_t^c$	Set of inflexible active power demand
$\boldsymbol{E}_i$	PoC to Bus mapping matrix for EVs
$\hat{\boldsymbol{E}}_i$	PoC to Bus mapping matrix for DGs
$\boldsymbol{D}$	Matrix of power transfer distribution factors
$\boldsymbol{Q}_t$	Set of Reactive Power demand on buses
$\boldsymbol{Z}$	Inverse of the partial nodal admittance matrix
$N_{\text{p},i}$	Number of PoC
$\boldsymbol{R}$	Real part of $\boldsymbol{Z}$
V_0	Voltage at the reference bus
N_{a}	Number of Aggregators
N_{T}	Number of time periods

Variables

f_i	Cost function of Aggregator i
$\boldsymbol{p}_{i,t}$	Set of active power of EV

$\hat{\boldsymbol{p}}_{i,t}$ Set of active power curtailment of DGs

$\boldsymbol{P}_t$ Set of total active power demand at hour t

$\boldsymbol{\tau}_{i,t}$ Set of DLMPs at EV PoC

$\hat{\boldsymbol{\tau}}_{i,t}$ Set of DLMP at DG PoC

$\bar{\boldsymbol{\tau}}_{i,t}$ Limit violation cost at EV PoC

$\hat{\bar{\boldsymbol{\tau}}}_{i,t}$ Limit violation cost at DG PoC

$\boldsymbol{\lambda}_t$ Set of line limit LMs

$\boldsymbol{\omega}_t$ Set of voltage limit LMs

$\boldsymbol{S}_t^k$ Set of subgradients

1. Introduction

The share of energy consuming distributed energy resources (DERs), such as electric vehicles (EVs), batteries and heat pumps, as well as generating DERs, such as wind turbines (WTs) and photovoltaics (PVs), otherwise called distributed generators (DGs), is increasing. This is driven by the growth of renewable energy resources and the electrification of the transportation and heating sectors. However, distribution networks (DNs) are not designed to accommodate those DERs, and a number of operational problems are expected to occur, as the share of DERs is increasing. Such problems are related to line overloading, mainly in urban networks, and voltage excursions in rural areas. This highlights the need for efficient DER management for DNs with large shares of such resources [1]. The role of the Distribution System Operators (DSOs) is crucial, requiring close cooperation with the owners and operators of DERs. Given the large amount and small capacities of individual DERs, aggregators, as market entities aiming to maximize their profits, will act as intermediates who manage portfolios of DERs [2].

The use of distribution locational marginal prices (DLMPs) has recently attracted attention, as an efficient way of scheduling DERs on a DN level [3]. DLMPs are essentially an extension of locational pricing on a distribution level. In [4], nodal pricing incentivizes loss minimization, whereas in [5] voltage limits are additionally considered. Game theory and loss reduction allocation are employed along with dynamic tariffs in [6]. In [7], dynamic tariffs take into account losses, generation from renewables and line limits. The authors in [8] identify the problem of congestion as a result of price responsiveness at the distribution level, and suggest simple day ahead (DA) tariffs, based on lagrange multipliers (LMs). In [8, 9, 10] the authors suggest an elegant approach, where the DLMP consists of the cost of line congestion and spot price. In [11], DLMPs are used with chance-constrained mixed integer programming. In [12], DLMPs are used with convexified AC-OPF and hierarchical dispatch, which involves both the transmission and the DN. The work of [13] presents a complete framework for Volt/VAR control, network reconfiguration and interactions with the wholesale market, employing DLMPs and linearized power flow models.

The authors of [10] propose that DSOs calculate the DLMPs by solving the global welfare maximization problem. Afterwards, the aggregators use these DLMPs to schedule their DERs in a way that line congestions are avoided. By using linear cost functions, the published DLMPs result in multiple solutions to the aggregators' optimization problems, which may lead to network violations [14]. This problem was overcome in [15], by considering quadratic objective functions for the aggregators, guaranteeing the uniqueness of the solution obtained by the DLMPs.

A key characteristic of the aforementioned works is that DLMPs are calculated by the DSO assuming full knowledge of the aggregators' individual subproblems. This poses implementation challenges in a liberalized markets setup, because aggregators would have to share all the information related to their optimization problems with the DSO. Distributed optimization can provide a solution to this problem, by retaining the aggregators' privacy and still achieving the optimal solution.

In [16, 17, 18], the authors build upon [10] and [15], and present a decentralized way of obtaining the optimal DLMPs, based on the dual decomposition method [19]. In this context, the aggregators and the DSO iteratively exchange schedules and DLMPs, until they converge to the optimal solution. Practical limitations, related to data privacy, dictate the use of a decentralized solution. This refers to a setup involving a coordinator (DSO) and agents (aggregators) communicating in a star topology. Implementing such a solution has two requirements. First, the overall optimization problem (the aggregators' problems and the DSO network constraints) has to be convex, to ensure that it can be decomposed. Survey [20] presents an extensive overview of linearization power flow methods, which are necessary to achieve this. Second, the required computational time to obtain the optimal solution must be relatively small, so that the method can be applicable.

In [15, 16, 17] the authors consider the line limits for the formulation of the DLMPs but not the voltage limits, whose violation is one of the most common problems in DNs. Ref. [18] considers voltage limits, but the effect of concepts such as the price sensitivity parameter, which is introduced in Section 2, on the resulting schedules is not discussed. Lower price sensitivity values result in *less convex* problems which are harder to converge. However, more realistic values are low, and therefore this issue must be addressed. In addition, violations in adjacent buses can slow down convergence, a case that can be met in larger radial networks with longer linear sections.

Works [15], [16], [17], and [18] consider consuming DERs and not generating DERs, whose synergies can maximize social welfare. The presence of generating DERs, and the resulting bidirectional power flows, affect not only the formulation of the problem but also its convergence speed. Problems with non-intertemporal decision constraints, which is the case with power curtailment, are much more sensitive to the choice of update steps in decentralized iterative solutions, and special consideration must be given.

The first contribution of this paper is the inclusion of generating DERs in the DLMP formulation, to capture the synergies from co-optimizing generating and consuming DERs under voltage constraints. We represent generating DERs by using the available power curtailment as a decision variable of the problem. The second contribution is a novel concept based on observations of the system topology, to significantly increase convergence speed in radial networks. More specifically, redundant LMs are identified and set to zero, leading to significant convergence acceleration. In addition, such an enhancement is generic, can be applied across all decentralised or distributed optimization methods to distribution networks and to the best of our knowledge has not been previously proposed. In addition, an active update step is employed, to overcome the convergence problems introduced by the presence of generating DERs, thereby further improving convergence speed. Finally, the role of the price sensitivity parameter, used in the aggregators' objective functions for obtaining a realistic model and behaviour of the system, is discussed. We validate our method by using a 33 bus system with multiple DERs, and we show that iterations can be reduced threefold compared to the state-of-the art, making the method applicable even for intraday operation [21].

The remainder of the paper is organized as follows. Section 2 presents the optimization problem and the iterative decentralized solution. In Section 3 the convergence speed improvement is discussed, and Section 4 presents the performed case studies and key results. Finally, Section 5 concludes the paper.

2. Problem formulation

2.1. DSO's problem

The aggregators use the forecasted DA spot prices to optimally schedule their DERs when they participate in the DA market. However, the scheduling of flexible demand has an impact on the electricity prices. To account for this effect, a spot price prediction method that relies on price sensitivity is proposed in [1], so that unrealistically high peaks in demand are avoided. We denote by c_t and p_t the forecasted baseline DA price and the active power demand at hour t, respectively. The resulting DA price is given by

$$y_t = c_t + \beta_t p_t. \tag{1}$$

As outlined in [1, 22], the electricity price is linearized around an average value, and then the sensitivity parameter β is estimated by using the merit order of the power plants. This approximation allows for structuring the aggregator's problem with a **Quadratic Programming (QP)** formulation by multiplying price y_t with the DER demand, as in [15]. We denote by $\boldsymbol{p}_{i,t}$ the active demand variable vector at time step $t \in N_{\mathrm{T}}$ for aggregator $i \in N_{\mathrm{a}}$, which is used as the decision variable assigned to the charging of EVs. To include generating DERs in the optimization problem, $\hat{\boldsymbol{p}}_{i,t}$ is used as a second decision variable, representing their active power curtailment, with regards to the forecasted value. This active power curtailment is a non-negative variable, as the EV charging. For the rest of the paper bold letters will denote vectors and $(\hat{\cdot})$ will refer to generating DERs. Thus, the objective function is similar as in [1, 15, 16, 18, 23], meaning of quadratic form, with a positive definite Hessian matrix. Since all constraints are affine, the problem becomes a strictly convex QP problem. The DSO's objective is to maximize social welfare, which is equivalent to maximizing the sum of the aggregators' profits. Since EVs, PVs and WTs are considered, the corresponding marginal costs are zero. Each aggregator's objective function is given by

$$f_i = \sum_{t=1}^{N_{\mathrm{T}}} \left[(\frac{1}{2}\boldsymbol{p}_{i,t}^T B_{i,t}\boldsymbol{p}_{i,t} + c_t\boldsymbol{p}_{i,t}) + (\frac{1}{2}\hat{\boldsymbol{p}}_{i,t}^T B_{i,t}\hat{\boldsymbol{p}}_{i,t} + c_t\hat{\boldsymbol{p}}_{i,t}) \right]. \tag{2}$$

The DSO's optimization problem is formulated as:

$$\min_{\boldsymbol{p}_{i,t},\hat{\boldsymbol{p}}_{i,t}} \sum_{i=1}^{N_{\mathrm{a}}} f_i, \tag{3}$$

subject $\forall\ i \in N_{\mathrm{a}}$ and $t \in N_{\mathrm{T}}$ to:

$$\boldsymbol{e}_{i,t}^{\min} \leq \sum_{\tau=1}^{t}(\boldsymbol{p}_{i,\tau} - \boldsymbol{d}_{i,\tau}) + \boldsymbol{e}_i^{\mathrm{init}} \leq \boldsymbol{e}_{i,t}^{\max} \qquad (\boldsymbol{\mu}_{i,t}^-, \boldsymbol{\mu}_{i,t}^+) \tag{4}$$

$$0 \leq \boldsymbol{p}_{i,t} \leq \boldsymbol{p}_{i,t}^{\max} \qquad (\boldsymbol{\sigma}_{i,t}^-, \boldsymbol{\sigma}_{i,t}^+) \tag{5}$$

$$0 \leq \hat{\boldsymbol{p}}_{i,t} \leq \hat{\boldsymbol{p}}_{i,t}^{\max} \qquad (\hat{\boldsymbol{\sigma}}_{i,t}^-, \hat{\boldsymbol{\sigma}}_{i,t}^+) \tag{6}$$

$$\boldsymbol{P}_t = \boldsymbol{P}_t^{\mathrm{c}} + \sum_{i=1}^{N_{\mathrm{a}}}(\boldsymbol{E}_i\boldsymbol{p}_{i,t} + \hat{\boldsymbol{E}}_i(\hat{\boldsymbol{p}}_{i,t} - \hat{\boldsymbol{p}}_{i,t}^{\max})) \qquad (\boldsymbol{\gamma}_t) \tag{7}$$

$$\underline{\boldsymbol{F}} \leq \boldsymbol{D}\boldsymbol{P}_t \leq \overline{\boldsymbol{F}} \qquad (\boldsymbol{\lambda}_t^-, \boldsymbol{\lambda}_t^+) \tag{8}$$

$$\underline{\boldsymbol{V}} \leq V_0(1 - \frac{1}{V_0^2}Re\{\boldsymbol{Z}\cdot(\boldsymbol{P}_t - j\boldsymbol{Q}_t)\}) \leq \overline{\boldsymbol{V}}.\ (\boldsymbol{\omega}_t^-, \boldsymbol{\omega}_t^+) \tag{9}$$

We denote by $\boldsymbol{d}_{i,t}$ and $\boldsymbol{e}_{i,t}$ the energy demand and state of charge (SoC) of the EVs respectively. Superscripts max, min and init refer to the maximum, minimum and initial values respectively. Further, $(\bar{\cdot})$ and $(\underline{\cdot})$ are used for the upper and lower limits of the parameters, respectively. $\boldsymbol{P}_t$, $\boldsymbol{Q}_t$ and $\boldsymbol{P}_t^{\mathrm{c}}$ refer to the total active, reactive and conventional (inflexible) active demand of a bus, respectively. $\boldsymbol{E}_i$ is a matrix mapping the point of connection (PoC) of EVs or generating DERs to the network's buses for aggregator i. $\boldsymbol{F}$ and $\boldsymbol{V}$ are the line loading and voltage limits, and $\boldsymbol{D}$ is the power transfer distribution factor (PTDF). V_0 is the reference bus voltage, $\boldsymbol{Z}$ the inverse of the partial nodal admittance matrix, and $B_{i,t}$ the block diagonal matrix of the price sensitivity parameter β. Managing uncertainty (e.g. by using scenarios or robust optimization) is an important task for both the aggregators and the DSOs. This is not considered in our formulation, but falls into the scope of our future work.

Next to each constraint, a greek letter is assigned to the associated dual variables, with superscripts $^+$ and $^-$ referring to the right-hand and left-hand constraints, respectively.

Constraints (4)-(6) are applied to each PoC, and (7)-(9) involve all the PoC and couple the aggregators' sub-problems. Constraint (4) refers to the EVs energy needs, considering their availability on each hour. Constraints (7)-(9) enforce the active power balance, the line and the voltage limits on each bus, respectively. The last constraint is based on the voltage approximation presented in [24], that provides higher accuracy in more resistive networks with power factors closer to unity.

2.2. Aggregator's sub-problem

The optimization problem of aggregator i is expressed as:

$$\min_{\boldsymbol{p}_{i,t},\hat{\boldsymbol{p}}_{i,t}} f_i, \tag{10}$$

subject $\forall\, t \in N_{\mathrm{T}}$ to constraints (4)-(6). In this paper, we assume that the aggregators are operating in an ethical manner, using accurate information and without trying to manipulate the market clearing process.

2.3. DLMP formulation

It is easy to notice that the DSO's problem (i.e., the global problem) consists of all of the aggregators' problems put together and the coupling constraints (7)-(9). We form the dual of the global problem using a partial Lagrangian that includes only the coupling constraints, because if the primal problem is convex, local duality can be defined with respect to any subset of the constraints [25]. This allows for the decomposition of the dual problem into sub-problems that do not have any coupling constraints, according to the dual decomposition method [19]. They only share the LMs in their objective function. These sub-problems are identical to the aggregator individual problems, save for the terms that include LMs in their objective function. The aggregators could find the optimal solution if they knew the optimal value of the LMs and, hence, the corresponding terms.

First, we will show how to find what terms to add to each aggregator's problem to make it identical to the sub-problem of the global problem. We start from the partial Lagrangian, whose gradient will give us those terms. These terms are the violation price shown later in this section. The partial Lagrangian of the global problem, considering only the coupling constraints, is equal to:

$$\begin{aligned} L(\boldsymbol{p}_{i,t},\hat{\boldsymbol{p}}_{i,t};\boldsymbol{\lambda}_t^{-,+},\boldsymbol{\omega}_t^{-,+}) = {} & \sum_{i=1}^{N_{\mathrm{a}}} f_i - \sum_{t=1}^{N_{\mathrm{T}}} \boldsymbol{\lambda}_t^{-}(\boldsymbol{D}\boldsymbol{P}_t - \underline{\boldsymbol{F}}) + \sum_{t=1}^{N_{\mathrm{T}}} \boldsymbol{\lambda}_t^{+}(\boldsymbol{D}\boldsymbol{P}_t - \overline{\boldsymbol{F}}) \\ & - \sum_{t=1}^{N_{\mathrm{T}}} \boldsymbol{\omega}_t^{-}(V_0[1 - \frac{1}{V_0^2} Re\{\boldsymbol{Z}\cdot(\boldsymbol{P}_t - j\boldsymbol{Q}_t)\}] - \underline{\boldsymbol{V}}) \\ & + \sum_{t=1}^{N_{\mathrm{T}}} \boldsymbol{\omega}_t^{+}(V_0[1 - \frac{1}{V_0^2} Re\{\boldsymbol{Z}\cdot(\boldsymbol{P}_t - j\boldsymbol{Q}_t)\}] - \overline{\boldsymbol{V}}). \end{aligned} \tag{11}$$

The DLMPs are given by the gradient of the partial Lagrangian. Details on the derivation of the DLMPs can be found in our previous work [21]. The DLMPs are assigned the symbols

$\boldsymbol{\tau}_{i,t}$ and $\hat{\boldsymbol{\tau}}_{i,t} \in \mathbb{R}^{N_{\mathrm{p},i} \times N_{\mathrm{T}}}$, $\forall\, i = 1, .., N_{\mathrm{a}}$ for consuming and generating DERs respectively. $N_{\mathrm{p},i}$ is the number of PoC of aggregator i, and the DLMPs are calculated as

$$\boldsymbol{\tau}_{i,t} = \frac{\partial L}{\partial \boldsymbol{p}_{i,t}} = c_t + B_{i,t}\boldsymbol{p}_{i,t} + \bar{\boldsymbol{\tau}}_{i,t}, \tag{12}$$

$$\hat{\boldsymbol{\tau}}_{i,t} = \frac{\partial L}{\partial \hat{\boldsymbol{p}}_{i,t}} = c_t + B_{i,t}\hat{\boldsymbol{p}}_{i,t} + \hat{\bar{\boldsymbol{\tau}}}_{i,t}, \tag{13}$$

where $\bar{\boldsymbol{\tau}}_{i,t}$ and $\hat{\bar{\boldsymbol{\tau}}}_{i,t}$ are the **violation price** components of the DLMP, and are given by

$$\bar{\boldsymbol{\tau}}_{i,t} = \boldsymbol{\lambda}_t^{+,-}(\boldsymbol{D}\boldsymbol{E}_i) - \boldsymbol{\omega}_t^{+,-}(\frac{\boldsymbol{R}\boldsymbol{E}_i}{V_0}), \tag{14}$$

$$\hat{\bar{\boldsymbol{\tau}}}_{i,t} = \boldsymbol{\lambda}_t^{+,-}(\boldsymbol{D}\hat{\boldsymbol{E}}_i) - \boldsymbol{\omega}_t^{+,-}(\frac{\boldsymbol{R}\hat{\boldsymbol{E}}_i}{V_0}). \tag{15}$$

A DLMP is composed of three parts:

- The predicted market price: $c_t + B_{i,t}\boldsymbol{p}_{i,t}$.
- The line congestion price: $\boldsymbol{\lambda}_t^{+,-}(\boldsymbol{D}\boldsymbol{E}_i)$.
- The voltage limit violation price: $-\boldsymbol{\omega}_t^{+,-}(\frac{\boldsymbol{R}\boldsymbol{E}_i}{V_0})$, where $\boldsymbol{R} = Re\{\boldsymbol{Z}\}$.

Price components $\bar{\boldsymbol{\tau}}_{i,t}$ and $\hat{\bar{\boldsymbol{\tau}}}_{i,t}$ can be calculated by using the LMs $\boldsymbol{\lambda}_t^{+,-}$ and $\boldsymbol{\omega}_t^{+,-}$, which are shared with the aggregators. The aggregator's new objective function, considering the violation prices, will be:

$$\tilde{f}_i = \sum_{t=1}^{N_{\mathrm{T}}} (\frac{1}{2}\boldsymbol{p}_{i,t}^T B_{i,t}\boldsymbol{p}_{i,t} + (c_t + \bar{\boldsymbol{\tau}}_{i,t})\boldsymbol{p}_{i,t}) + \sum_{t=1}^{N_{\mathrm{T}}}(\frac{1}{2}\hat{\boldsymbol{p}}_{i,t}^T B_{i,t}\hat{\boldsymbol{p}}_{i,t} + (c_t + \hat{\bar{\boldsymbol{\tau}}}_{i,t})\hat{\boldsymbol{p}}_{i,t}). \tag{16}$$

By incorporating the violation prices into the aggregators' problems, the DSO problem and the new aggregators' problems put together become equivalent, as described in [21]. Therefore, if the aggregators receive and incorporate the violation prices $\bar{\boldsymbol{\tau}}_{i,t}$ and $\hat{\bar{\boldsymbol{\tau}}}_{i,t}$ in their objective functions, the obtained solution will be the same as the **centralized solution** of the DSO problem. This provides a way of obtaining the optimal global solution via the individual aggregator subproblems, if one already knows the optimal LMs.

One way to obtain the optimal LMs is if the aggregators send to the DSO all the information necessary to construct the individual optimization problems. Then, the DSOs could calculate and communicate the violation prices to the aggregators, who would then schedule their DERs by taking them into account. However, it is preferable that such sensitive information is not shared. A distributed solution where the optimal LMs are obtained iteratively is preferred. In this framework the aggregators only send their schedules to the DSOs at each iteration. For simplicity, DLMPs obtained with the iterative decentralized solution will be called iDLMPs [16].

2.4. iDLMPs

In the iDLMPs context, the projected subgradient method is applied to solve the decomposed problem by obtaining the optimal LMs iteratively [19]. Fig. 1 illustrates this process. First, the DSO initialises the LMs and sends the violation prices to the aggregators. Next, the aggregators solve their individual optimization problems (16), subject to constraints (4)-(6), and send their schedules to the DSO. The DSO uses the new schedules to update the LMs by using (18) and (19). See how (18) and (19) make use of equation (17), which in turn needs these new aggregator schedules. This process is repeated until the LMs converge.

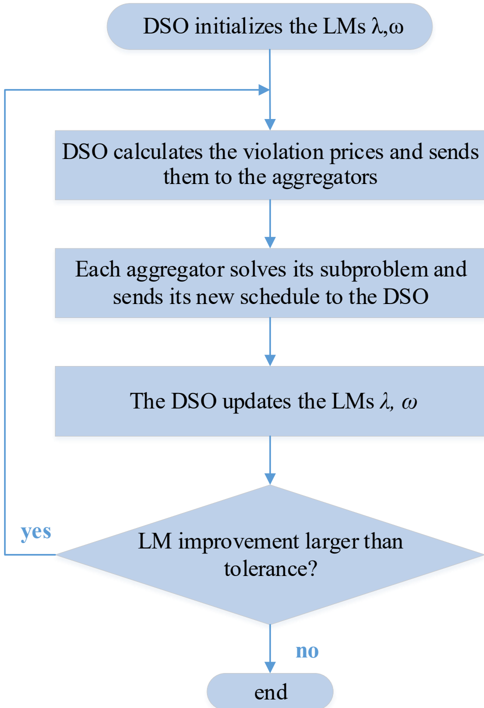

Figure 1: Flow chart outlining the fundamental steps of the iterative process.

The LMs are updated at each iteration k by calculating the subgradient terms $\boldsymbol{S}_t^k$ for each time step t. A more detailed description of this process can be found in [19], [21]. Subgradients $\boldsymbol{S}_t^k$ are calculated as

$$\begin{bmatrix} \boldsymbol{S}_t^{\lambda^+;k} \\ \boldsymbol{S}_t^{\lambda^-;k} \\ \boldsymbol{S}_t^{\omega^+;k} \\ \boldsymbol{S}_t^{\omega^-;k} \end{bmatrix} = \begin{bmatrix} -(\boldsymbol{DP}_t^k - \overline{\boldsymbol{F}}) \\ \boldsymbol{DP}_t^k - \underline{\boldsymbol{F}} \\ -V_0[1 - \frac{1}{V_0^2} Re\{\boldsymbol{Z} \cdot (\boldsymbol{P}_t^k - j\boldsymbol{Q}_t)\}] + \overline{\boldsymbol{V}} \\ V_0[1 - \frac{1}{V_0^2} Re\{\boldsymbol{Z} \cdot (\boldsymbol{P}_t^k - j\boldsymbol{Q}_t)\}] - \underline{\boldsymbol{V}} \end{bmatrix} \tag{17}$$

The LMs are updated at each iteration k by using the projection onto the non-negative orthant, which is denoted by $(\cdot)_+$, according to:

$$\boldsymbol{\lambda}_t^{+,-;k+1} = (\boldsymbol{\lambda}_t^{+,-;k} + \boldsymbol{\alpha}_t^{\lambda} \boldsymbol{S}_t^{\lambda+,-;k})_+, \ \forall t \in N_{\mathrm{T}} \tag{18}$$

$$\boldsymbol{\omega}_t^{+,-;k+1} = (\boldsymbol{\omega}_t^{+,-;k} + \boldsymbol{\alpha}_t^{\omega} \boldsymbol{S}_t^{\omega+,-;k})_+, \ \forall t \in N_{\mathrm{T}} \tag{19}$$

where $\boldsymbol{\alpha}_t^{\lambda}$ and $\boldsymbol{\alpha}_t^{\omega}$ are small and constant positive steps to guarantee convergence [19].

3. Improving convergence speed

As discussed in Section 2, the convergence of the subgradient method is guaranteed for a small positive update step. However, low convergence speed can hinder any practical application of the method. In our investigation we identified two issues that might slow down convergence. The first issue occurs when the initial limit violations are small. This leads to small subgradient terms and slow convergence when a constant step is used, especially as the algorithm progresses and the subgradient term decreases further. Therefore, a classic dilemma arises: a very small step size results in a slow convergence, whereas a very large step size may lead to quite erratic fluctuations. In practice, it is difficult to choose a constant step size that has good convergence properties for both the early and late stages of the algorithm.

A diminishing step size, such as α/k or $\alpha/\sqrt{k}$, can be an improvement. However, this results in a decrease of the step size even when progress towards the optimum is made. Therefore, we employ an *active* step, inspired by [26], for each LM, of the following form: $\alpha/(\kappa_t + 1)$. $\kappa_t < k$ is the number of iterations prior to k, where the value of the specific LM decreases. In [26], it is suggested that the value of the Lagrangian is used as the criterion for increasing κ_t. However, each LM may converge to its optimal value at a different rate. To achieve smoother and faster convergence, we apply the aforementioned rule on each LM separately.

The second issue is linked to constraint (9). For illustrating purposes only, assume there is no generation in a radial DN, see Figure 2. As we move towards the end of a *non-branching* section (e.g. from $k-5$ to k), one bus at a time, each voltage constraint (9) defines a continuously narrower solution space. This means that the voltage constraints associated with all but the last bus are non-binding. Therefore, all voltage-related LMs, $\boldsymbol{\omega}_t^{-,*}$, corresponding to the optimal solution, will be certainly zero on all but the last bus (bus k. This is a property of radial DNs that we can take advantage of.

Now, let us keep the assumption that we have a radial DN with no generation. The iterative procedure is inherently flawed. The LMs are updated by the subgradient of the dual problem, see (17). During the procedure, it is possible that voltage limits are violated on a number of buses along a non-branching section of the grid. This leads to LMs $\boldsymbol{\omega}_t^{-}$ on those buses starting to increase iteration after iteration. However, as we explained, only the last buses can have non-zero voltage LMs at the optimal solution. As we observed in our simulations, the rest of the voltage LMs will increase at first, and then start decreasing until they become zero, by the time the method converges to the optimal solution. In that sense, these LMs are redundant to the solution of the problem, and can slow down convergence

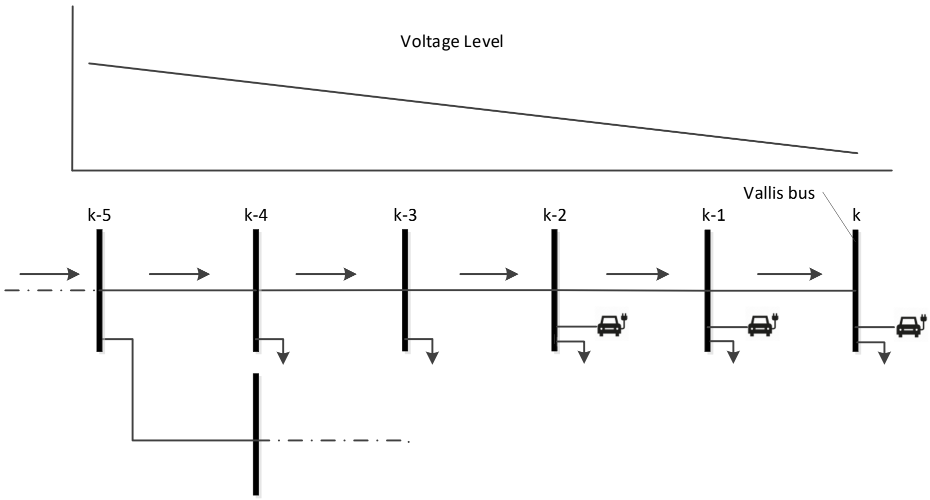

Figure 2: An example of a non-branching section of DN with only consuming resources and qualitatively the corresponding voltage level.

significantly. To speed up convergence, they can be fixed to zero throughout the whole process.

A bus that will have a non-zero $\boldsymbol{\omega}_t^-$ at the optimal solution will be called a *vallis* bus. Such a bus will always have the lowest voltage level in its vicinity. The opposite is a bus with the highest voltage level in its vicinity. We call such a bus *collis*, and is associated with a non-zero $\boldsymbol{\omega}_t^+$. Such a bus can occur with a generating unit sending power to the reverse of the conventional direction, see the fixed generation on Figure 3.

One can easily identify the vallis bus as the last bus on a non-branching section, when only consuming DERs are considered, as in previous related works such as [16, 17, 18]. In that case, collis buses will not exist. However, in the presence of generating units it is not straightforward to identify collis or vallis buses. This is due to reverse power flows that may result in voltage levels alternating between increasing and decreasing across a single non-branching section, see Figure 3. Again for illustrative purposes, note that, unlike the PV plant on bus $k-1$ which is dispatched through the iDLMP method, the plant on bus k has a fixed output. In other words, it is impossible to identify with certainty which buses are collis or vallis, because the iDLMP method will affect the power injection on each bus, potentially changing which buses are collis or vallis at the end. Therefore, to be on the safe side, we would like to know where reverse power flows occur, and consider all the relevant buses as candidates collis/vallis.

To do so, we exploit another property of the method. Both decision variables point to the same direction regarding power injection on a bus. This means that increasing EV charging or generating DERs curtailment will decrease active power injection on a bus (equivalently increase consumption). Thus, starting from the initial case where both decision variables ($\mathbf{p}_{i,t}^*$, $\hat{\mathbf{p}}_{i,t}^*$) are equal to zero, any reverse power flows can only get shorter than that, during the execution of the method, meaning that they extend to less buses than initially. In Figure 3, if EVs charge more or PVs have their power curtailed more, there will be less power sent

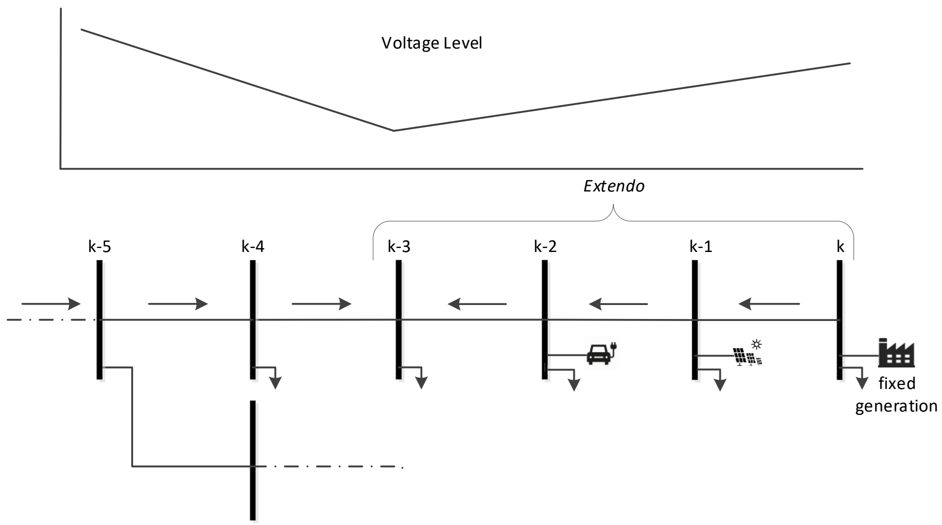

Figure 3: An example of a non-branching section of DN with both consuming and generating DER and qualitatively the corresponding voltage level.

towards bus $k-3$, potentially to the point where power flow between $k-3$ and $k-2$ will change direction pointing to the right, thus shortening the *extendo* up to $k-2$. By extendo we call the group of adjacent buses a reverse power flow can affect. The opposite, however, cannot happen, meaning we have no way of lengthening the extendo beyond bus $k-3$. Therefore, before actually executing the iDLMP method, we know which buses to add as candidate collis or vallis (those affected by reverse power flows in the initial case).

The reverse active power flows are calculated by employing the linearized DistFlow equations [27]. We assume a DN is radial, and that reactive power is strictly consumed anywhere in the grid. Thus, any loss of accuracy from the method is towards the safe side (reactive consumption on a bus shortens the reverse power flow extend). We calculate the active power flows by using the following equation from the linearized DistFlow method:

$$P_{lm} = -P_m + \sum_{n:m\to n} P_{mn}. \tag{20}$$

According to (20), the active power flowing from bus l to bus m is equal to the sum of active power flows from m to the rest adjacent buses and the active power injection at bus m, see (7). We group adjacent lines that have reverse power flows to form the extendo of a reverse power flow. All the buses in an extendo are affected by a reverse power flow occurrence, and are candidate collis and vallis. In Fig. 4 the process of the collis/vallis buses identification is outlined.

4. Case Studies

4.1. Test system and parameters

The test system used is the Baran-Wu 33 Bus Network [28], shown in Fig. 5. It is a 12.66 kV network with five looping lines, which in the simulations are assumed to be open.

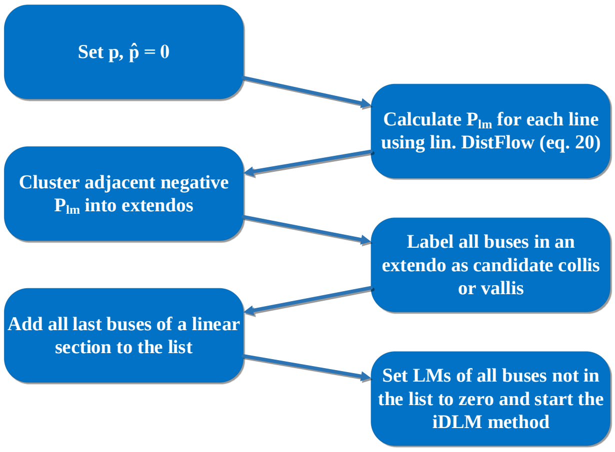

Figure 4: Outline of the process identifying vallis and collis buses for each linear section of a radial DN.

The critical lines to be examined in the results have a limit of ±1.1 MW and the allowed voltage violation is ±6%, as in [18]. The reactive power consumption is 10% of the active power, similar to [18]. For the baseline prices c_t, typical Elspot prices for Denmark's eastern power system (DK2) on a summer day were used, and the conventional consumption pattern was that of [10]. The prices are hourly, and so is the optimization time step. For the PV production, a simple summer pattern corresponding to Denmark was used, and for the WT production, data from a typical summer day were retrieved from a WT installed in a DN in Denmark, see Fig. 6. We assume two aggregators exist, having eight EV, four PV and four WT PoC each. EV capacity is 30 kWh with peak charging power of 3.7 kW. The minimum and maximum allowed SoC are 30% and 85%, respectively, and the final SoC is greater than or equal to the initial SoC. Each EV fleet consists of 100 EVs. The EV driving and consumption patterns were retrieved from [29]. Each PV and WT installation at a PoC is a power plant of 200 kW solar or wind power, respectively.

For the price sensitivity parameter β, a value of 1 €/MWh^2 is chosen. This leads to a realistic system behavior regarding the effect of DER scheduling on system prices, as demonstrated in subsection 4.3. All simulations were performed in **MATLAB**, using the **YALMIP** framework [30] and **Gurobi** [31] as a solver. **MATPOWER** [32] was used for the load flow calculations.

4.2. Case studies results

4.2.1. 33 bus test system

We start by optimizing the aggregators' schedules without applying DLMPs, thus neglecting the network's constraints (*without DLMPs case*). Then, the method is applied (*with DLMPs case*) and the results are compared with respect to line and voltage limit violations. It is noted that whether results are obtained using the centralized variant or the decentralized iDLMPs method is not an issue, as the two come to identical solutions, i.e. the unique optimal solution of the global problem. Fig. 7 shows the effectiveness of DLMPs regarding

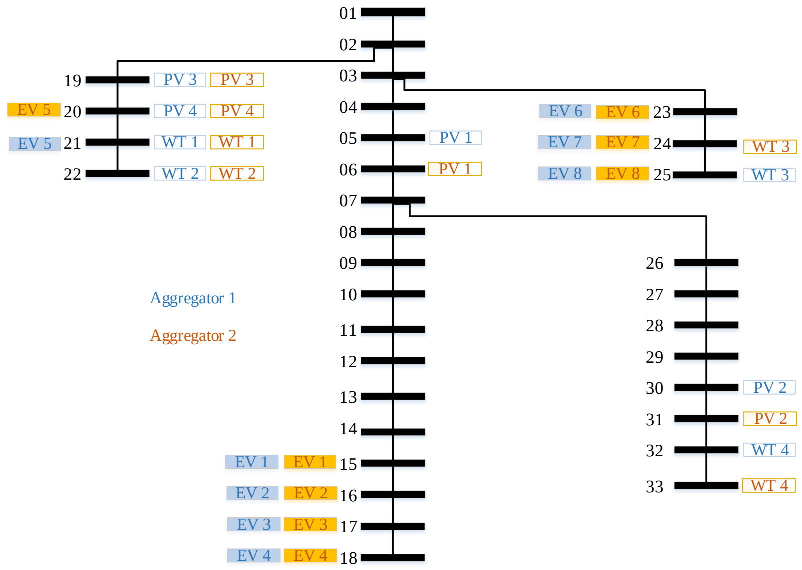

Figure 5: 33 bus test system, showing the DERs at their PoC.

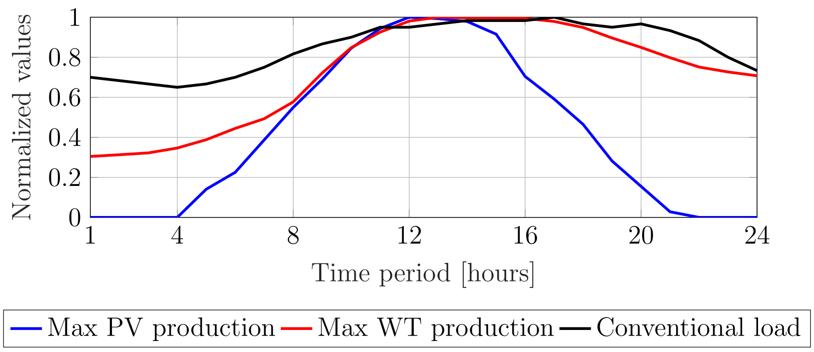

Figure 6: Forecasted patterns: PV and WT maximum output, and load.

line loading violations. The method instructs rescheduling of EV charging and curtailment of PV and WT production so that all limits are respected.

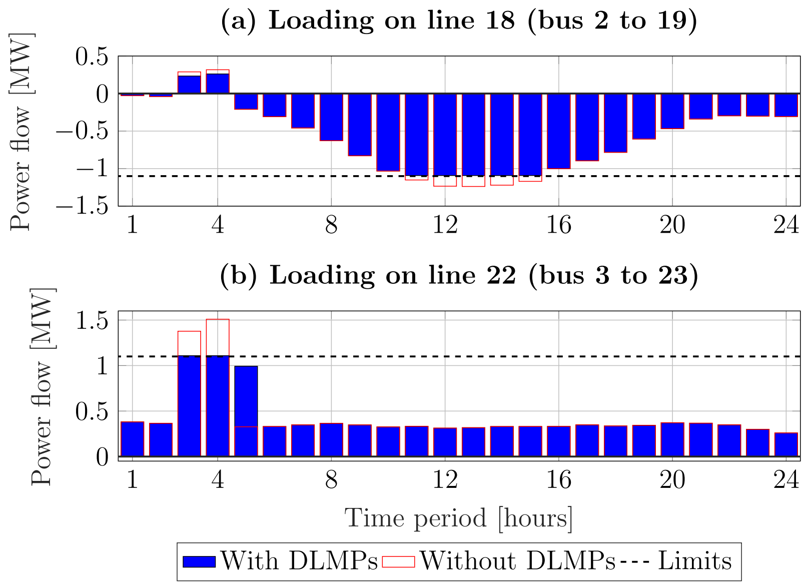

Figure 7: Line loadings with and without DLMPs.

Fig. 8 depicts how voltage profiles are improved by the implementation of the method. EV charging is spread throughout the night hours, namely from the 23rd to the 5th, instead of occurring mainly at the 3rd and 4th hours. The results are obtained by solving the AC power flow, and not by using the approximation model [24], to demonstrate the validity of the method. To avoid exceeding the line limits in hours $11-15$ due to excessive renewable production, the DSO would have to curtail PV and WT output. In the absence of DLMPs, curtailment is applied proportionally to all generating DERs along each linear section of the system, e.g. buses 19-22.

Fig. 9 illustrates how instead of curtailing some of PV and WT output (blue curve), this energy is used to charge a neighbouring fleet of EVs (red curve). This energy is essentially free of charge, as the produced DLMP is marginally negative, to render power generation unprofitable. The EV fleet on this bus takes advantage of this new locational price and changes the EV schedules to charge as much as possible on such an hour.

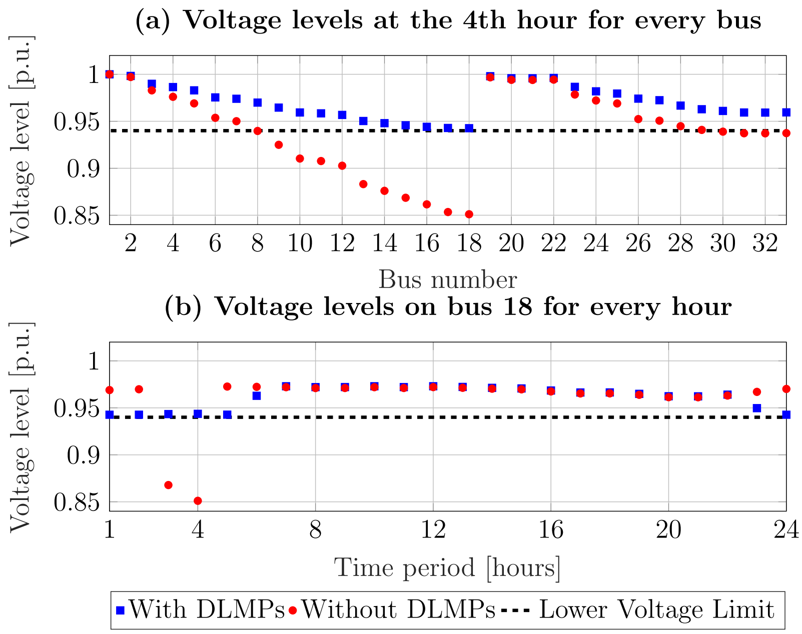

Figure 8: Voltage levels with and without DLMPs.

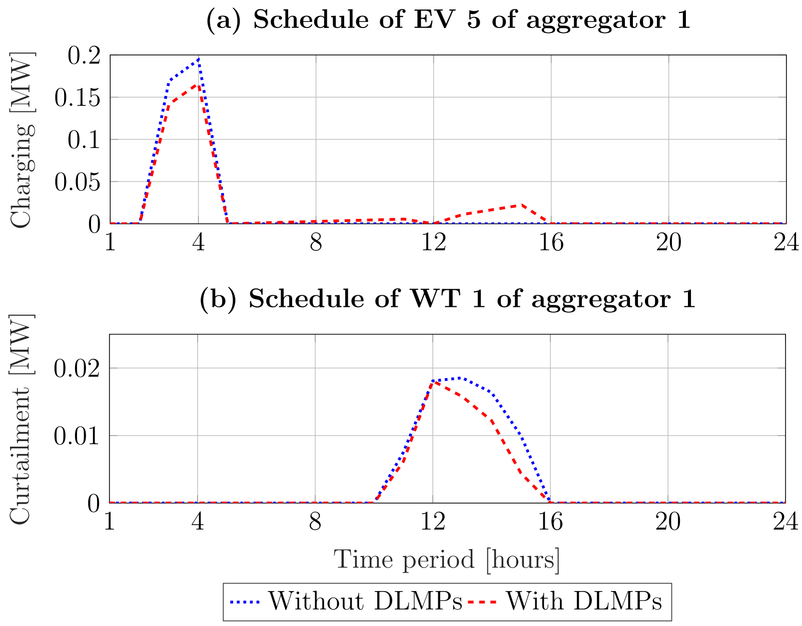

Figure 9: EV charging and WT curtailment with and without DLMPs.

Fig. 10 depicts the convergence of four of the most critical LMs, using the proposed collis-vallis identification process and the active steps $\boldsymbol{\alpha}_t/(\boldsymbol{\kappa}_t+1)$. Two of the presented LMs are associated with line limits violations, and two with voltage limits. It is observed that convergence is smooth and 225 iterations are required for the LMs to converge (with a tolerance of 0.001), which is acceptable for the method to have practical application. Using larger values of $\boldsymbol{\alpha}_t$ will only result in erratic fluctuations of the LMs.

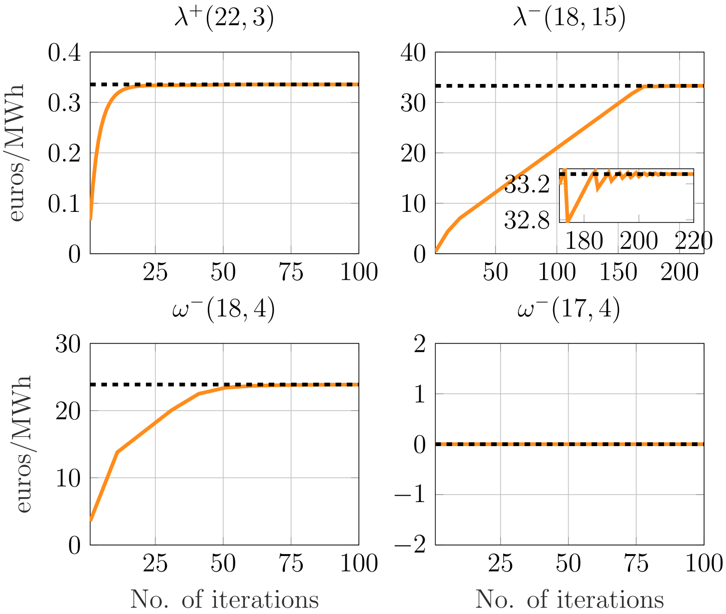

Figure 10: Convergence of four LMs when the vallis-collis concept is employed. Dashed lines represent the centralized solution and solid curves the values from the decentralized implementation.

To illustrate the significance of identifying the collis-vallis buses, we repeated the simulations using fixed step sizes (equations (18) and (19)), and we don't set the respective non-candidate vallis and collis LMs to zero. In this case the method does not converge even after 600 iterations, given the same tolerance. In Fig. 11, one can observe why convergence is slowed down. LM $\boldsymbol{\omega}^-(17, 4)$ on bus 17 increases in the beginning of the method, before it starts decreasing at a very slow pace. Larger step values do not improve convergence speed, whereas smaller values of $\boldsymbol{\alpha}_t$ would have resulted in a less steep slope and even slower convergence.

Increasing the step sizes leads to fluctuations that prohibit convergence, as seen for $\boldsymbol{\lambda}^-(18, 5)$ in Fig. 11. LMs associated with line violations caused by generating DERs are very sensitive to the subgradient term (17) for low values of β. In other words, when the objective function is less convex. For violations caused by EVs, the intertemporal constraints act as a damping factor. A change in $\boldsymbol{\omega}^-$ will have a small impact on schedules because price differences between hours are small. For PVs and WTs, on the other hand, small changes on $\boldsymbol{\lambda}_t^{+,-}$ will affect the schedules for the next iteration significantly, creating a fluctuation effect that prohibits convergence, see the detail in Fig. 11. Therefore, it is evident that a type of step is needed, that will slow down the update speed when reaching the optimal LM.

Employing a proportional-integral (PI) diminishing step, as proposed in [18], does improve convergence speed, see Table 1. However, for high values of integral gains, fluctuations occur in the early iterations. Its performance is a trade-off between convergence speed and acceptable fluctuation intensity. A benefit of using the active step sizes is that they are more robust to parameter selection, because unlike the integral diminishing step, it actively adapts according to how convergence progresses. Therefore, the DSO is relieved from the burden of fine-tuning those parameters for each day and each DN, depending on the particular conditions of the optimization problem. With active step sizes, larger gains can be used more safely and achieve faster convergence, due to the adaptive properties of the method. See for instance Fig. 10, where using $\boldsymbol{\alpha}_t/(\boldsymbol{\kappa}_t+1)$ does not allow the fluctuations to persist, so a larger $\boldsymbol{\alpha}_t$ is used to achieve a steeper rise.

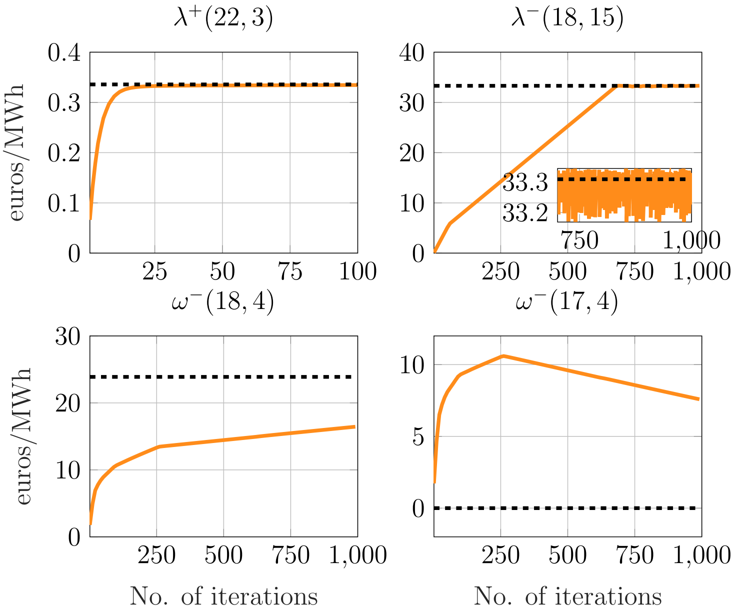

Figure 11: Convergence of four LMs when the vallis-collis concept is not employed.

The computational time depends mainly on the number of iterations, since the aggregators' optimization problems are simple to solve. In our case, approximately 30 iterations were executed per minute, but the optimization problems were solved sequentially and not in parallel, as would be the case in practice. In a real application with parallel execution, delays introduced by the communication links and the participants' infrastructure would constitute a major part of execution time, which is the reason we believe it is important to significantly reduce the number of the required iterations. Moreover, such a reduction allows for using the iDLMPs method with similar formulation for intra-day rescheduling, as suggested in [21], thus providing a more complete framework.

	Fixed step	**PI step of [18]**	**Prop. method**
Iter.	>1000	661	225

Table 1: Comparison: fixed step, PI step [18], and the proposed method.

4.2.2. 136 bus test system

The validity of the proposed method is tested with a larger test case. A 136-bus test system [33] is used, where 64 DER PoCs are considered. DERs are spread throughout the network and on critical hours there are network violations, with those of lower voltage limits being the more severe. Fig. 12 shows the convergence of the LMs of the bus with the most severe violation (bus 62) and its preceding bus (61), when the method is applied with and without the acceleration improvement. The same effect that was observed in the smaller test case is present here as well, slowing down convergence. It takes 226 iterations for convergence with the proposed method, compared to over well 1000 without it.

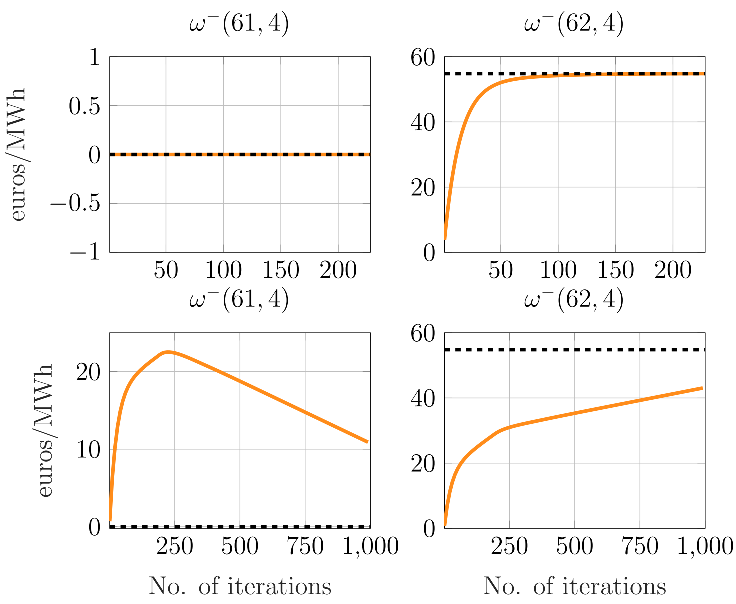

Figure 12: Convergence of four LMs with (up) and without (down) the vallis-collis concept for the 136-bus test case.

The size of the network does not directly impact convergence speed, because convergence is mostly affected by the severity of the violations. However, a larger network with more DER PoCs is possible to have more violations in the absence of coordination, like the iDLMP method. For example, in this case study, for bus 62 a little over 200 iterations were required to achieve convergence using the proposed method, while for the second most critical bus, a little over 150 iterations were needed. The more cases of violation there are, the more likely it is for a more "difficult-to-converge" bus, to occur. Without convergence acceleration, the required iterations were over one thousand.

4.3. Price sensitivity parameter effect

In [17] and [18] values above 50 €/MWh^2 are used. In the analysis performed in [34], the value of 0.015 €/MWh^2 is given as the price sensitivity to electricity demand. These differences found in the literature explain why one must be careful when choosing β, in

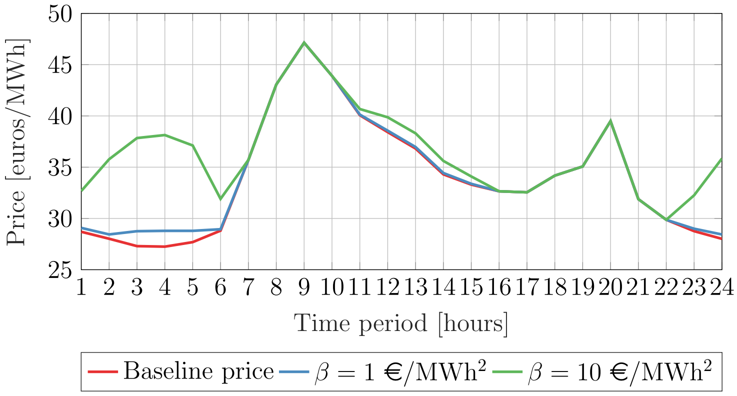

Figure 13: Projected prices compared with the baseline DA prices for different values of β.

order to obtain realistic results. The choice of β depends on the amount of flexible load used in each case study, see (1). We want the effect of DER scheduling to be as realistic as possible. We believe that the effect of DERs scheduling will be to a large extent forecasted and included in the baseline prices. To demonstrate the congestions that are occurring in present and near future DNs, we assume a significant presence of DERs in the studied DN but not prevalent in the overall power system. Therefore, we would not expect to see a very large sensitivity of electricity prices from DER scheduling.

In Fig. 13, we project the prices that will be formed after executing the method and scheduling the DERs. One observes that for larger values of β, the effect the EVs have on the resulting price is significant. Such an effect on prices is considered unrealistic for the present and the near future. Therefore, smaller values for β should be preferred. In our case studies a value of 1 €/MWh^2 was used. However, this tends to slow down convergence, as previously showcased. The combination of small and realistic β values, together with the presence of consuming DERs, complicate the convergence of iDLMPs, making convergence speed a particularly relevant problem. We believe that further research is necessary to identify what price sensitivity values are more accurate and realistic.

4.4. Accuracy of power flow linearization

Fig. 14 shows the voltage levels on every bus at the most critical hour, corresponding to Fig. 8, calculated using AC power flow and the linear approximation (9). One can see that even in these stressed conditions, the linear approximation performs well, with the maximum deviation from the real values being 0.8%. Due to an overestimation of voltage, the corresponding limits were slightly increased to 0.945, so that the actual voltage values from the AC calculations respect the voltage constraints.

5. Conclusion

We presented an iterative, decentralized method to alleviate line congestions and voltage problems in DNs, when both generating and consuming DERs are considered. We showed

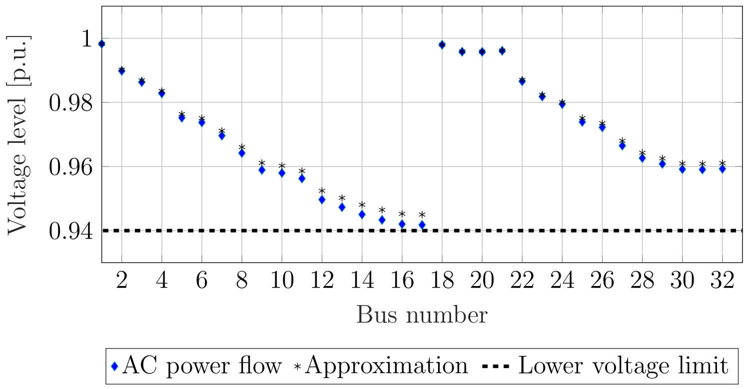

Figure 14: Voltage levels on every bus at the 4th hour calculated with AC power flow and the linear approximation of [24].

that by co-optimizing such resources, the otherwise curtailed PV and WT power can be used for EV charging, leading to an increase of social welfare. However, the presence of both types of resources and the use of small, realistic price sensitivity values significantly increases the number of required iterations. This may render a decentralized implementation of DLMPs impractical. We addressed this issue by proposing a novel concept based on topological information to increase convergence speed on radial DNs. This is achieved by identifying redundant constraints and setting the corresponding LMs to zero. Additionally, an active step size is used in the subgradient method to further accelerate convergence. Simulation results showed that these considerations can reduce the amount of required iterations by at least three times. This can make the implementation of such algorithms much more reliable for practical implementation. Finally, the concept of redundant constraints elimination can be applied to other decentralized algorithms for control and powers systems applications.

References

[1] R. A. Verzijlbergh, L. J. De Vries, Z. Lukszo, Renewable energy sources and responsive demand. Do we need congestion management in the distribution grid?, IEEE Trans. Power Syst. 29 (5) (2014) 2119–2128.

[2] S. Burger, J. P. Chaves-Ávila, C. Batlle, I. J. Pérez-Arriaga, The value of aggregators in electricity systems, MIT Center for Energy and Environmental Policy Research.

[3] A. Papavasiliou, Analysis of distribution locational marginal prices, IEEE Trans. on Smart Grid 9 (5) (2018) 4872–4882. doi:10.1109/TSG.2017.2673860.

[4] P. M. Sotkiewicz, J. M. Vignolo, Nodal pricing for distribution networks: efficient pricing for efficiency enhancing dg, IEEE Trans. Power Syst. 21 (2) (2006) 1013–1014. doi:10.1109/TPWRS.2006.873006.

[5] R. K. Singh, S. Goswami, Optimum allocation of distributed generations based on nodal pricing for profit, loss reduction, and voltage improvement including voltage rise issue, Int. J. Elec. Power 32 (6) (2010) 637–644.

[6] K. Shaloudegi, N. Madinehi, S. H. Hosseinian, H. A. Abyaneh, A novel policy for locational marginal price calculation in distribution systems based on loss reduction allocation using game theory, IEEE Trans. Power Syst. 27 (2012) 811–820.

[7] G. T. Heydt, B. H. Chowdhury, M. L. Crow, D. Haughton, B. D. Kiefer, F. Meng, B. R. Sathyanarayana,

Pricing and control in the next generation power distribution system, IEEE Trans. on Smart Grid 3 (2) (2012) 907–914.

[8] N. O Connell, Q. Wu, J. Østergaard, A. Nielsen, S. Cha, Y. Ding, Day-ahead tariffs for the alleviation of distribution grid congestion from electric vehicles, Elect. Power Syst. Res. 92 (2012) 106—114.

[9] F. Meng, B. H. Chowdhury, Distribution lmp-based economic operation for future smart grid, in: IEEE Power and Energy Conf. at Illinois, 2011, pp. 1–5. doi:10.1109/PECI.2011.5740485.

[10] R. Li, Q. Wu, S. S. Oren, Distribution locational marginal pricing for optimal electric vehicle charging management, IEEE Trans. Power Syst. 29 (1) (2014) 203–211.

[11] Z. Liu, Q. Wu, S. S. Oren, S. Huang, R. Li, L. Cheng, Distribution locational marginal pricing for optimal electric vehicle charging through chance constrained mixed-integer programming, IEEE Trans. on Smart Grid 9 (2) (2018) 644–654. doi:10.1109/TSG.2016.2559579.

[12] Z. Yuan, M. R. Hesamzadeh, D. R. Biggar, Distribution locational marginal pricing by convexified acopf and hierarchical dispatch, IEEE Trans. on Smart Grid 9 (4) (2018) 3133–3142. doi:10.1109/TSG.2016.2627139.

[13] L. Bai, J. Wang, C. Wang, C. Chen, F. Li, Distribution locational marginal pricing (dlmp) for congestion management and voltage support, IEEE Trans. Power Syst. 33 (4) (2018) 4061–4073. doi:10.1109/TPWRS.2017.2767632.

[14] W. Liu, F. Wen, Discussion on "distribution locational marginal pricing for optimal electric vehicle charging management", IEEE Trans. Power Syst. 29 (4) (2014) 1866–1866.

[15] S. Huang, Q. Wu, S. S. Oren, R. Li, Z. Liu, Distribution locational marginal pricing through quadratic programming for congestion management in distribution networks, IIEEE Trans. Power Syst. 30 (4) (2015) 2170–2178.

[16] S. Hanif, T. Massier, H. B. Gooi, T. Hamacher, T. Reindl, Cost optimal integration of flexible buildings in congested distribution grids, IEEE Trans. Power Syst. 32 (3) (2017) 2254–2266. doi:10.1109/TPWRS.2016.2605921.

[17] S. Hanif, H. B. Gooi, T. Massier, T. Hamacher, T. Reindl, Distributed congestion management of distribution grids under robust flexible buildings operations, IEEE Trans. Power Syst. 32 (6) (2017) 4600–4613. doi:10.1109/TPWRS.2017.2660065.

[18] S. Huang, Q. Wu, H. Zhao, C. Li, Distributed optimization-based dynamic tariff for congestion management in distribution networks, IEEE Trans. on Smart Grid 10 (1) (2019) 184–192. doi:10.1109/TSG.2017.2735998.

[19] S. Boyd, L. Xiao, A. Mutapcic, J. Mattingley, Notes on decomposition methods, Stanford University (2007) 1–36.

[20] D. K. Molzahn, F. Dörfler, H. Sandberg, S. H. Low, S. Chakrabarti, R. Baldick, J. Lavaei, A survey of distributed optimization and control algorithms for electric power systems, IEEE Trans. on Smart Grid 8 (6) (2017) 2941–2962. doi:10.1109/TSG.2017.2720471.

[21] P. Pediaditis, Optimization and control for integrating large shares of distributed energy resources in the distribution network, Master's thesis, Technical University of Denmark (2017).

[22] R. Verzijlbergh, Z. Lukszo, M. Ilic, Comparing different ev charging strategies in liberalized power systems, 2012 9th International Conference on the European Energy Market (EEM) (2012) 1–8.

[23] S. Huang, Q. Wu, Dynamic subsidy method for congestion management in distribution networks, IEEE Trans. on Smart Grid 9 (3) (2018) 2140–2151. doi:10.1109/TSG.2016.2607720.

[24] S. Bolognani, S. Zampieri, On the existence and linear approximation of the power flow solution in power distribution networks, IEEE Trans. Power Syst. 31 (1) (2016) 163–172.

[25] Y. Y. David G. Luenberger, Linear and Nonlinear Programming, 3rd Edition, International Series in Operations Research & Management Science, Springer, 2010.
URL `http://gen.lib.rus.ec/book/index.php?md5=BD6D3A33FC3EFE526C87013615D56724`

[26] A. M. Rush, M. Collins, A tutorial on dual decomposition and lagrangian relaxation for inference in natural language processing, J. Artif. Intell. Res. 45 (2012) 305–362. doi:10.1613/jair.3680.

[27] M. Baran, F. F. Wu, Optimal sizing of capacitors placed on a radial distribution system, IEEE Trans. Power Del. 4 (1) (1989) 735–743. doi:10.1109/61.19266.

[28] E. M. Baran, F. F. Wu, Network reconfigurationin distribution systems for loss reduction and load balancing, IEEE Trans. on Power Del. 4 (99) (1989) 1401–1407.

[29] Z. Liu, Q. Wu, L. Christensen, A. Rautiainen, Y. Xue, Driving pattern analysis of nordic region based on national travel surveys for electric vehicle integration, J. Mod. Power Syst. Clean Energy 3 (2) (2015) 180–189. doi:10.1007/s40565-015-0127-x.

[30] J. Löfberg, Yalmip : A toolbox for modeling and optimization in matlab, in: CACSD Conference, Taipei, Taiwan, 2004.

[31] G. Optimization, Gurobi Optimizer Reference Manual, Gurobi Optimization, Inc, Texas, 3rd Edition, gurobi Optimization (2010).

[32] R. D. Zimmerman, C. E. Murillo-Sanchez, Matpower: A matlab power system simulation package, Tech. rep., PSERC (2016).

[33] C. A. C. Marcos A.N. Guimaraes, Reconfiguration of Distribution Dystems for Loss Reduction Using Tabu Search, 15th Power System Computation Conference - PSCC 1 (2005) 1–6.

[34] T. K. Kristoffersen, K. Capion, P. Meibom, Optimal charging of electric drive vehicles in a market environment, Appl. Energy 88 (5) (2011) 1940 – 1948. doi:https://doi.org/10.1016/j.apenergy.2010.12.015.